MEASURING OPTICAL PROPERTIES ON ROUGH AND LIQUID METAL SURFACES

Authors:

M. Schmid, S. Zehnder, P. Schwaller, B. Neuenschwander, M. Held,
U. Hunziker, J. Zürcher

Corresponding author: M. Schmid

         e-mail: marc.schmid@bfh.ch

MEASURING OPTICAL PROPERTIES ON ROUGH AND LIQUID METAL SURFACES

M. Schmid, S. Zehnder, P. Schwaller, B. Neuenschwander, M. Held, U. Hunziker, J. Zürcher

Institute for Applied Laser, Photonics and Surface Technologies ALPS, Bern University of Applied Sciences, Pestalozzistrasse 20, 3400 Burgdorf, Switzerland

Abstract

For understanding and optimizing laser processing of metals and alloys the optical properties, especially the absorption of the work piece in function of the temperature up to the liquid phase have to be known [1]. There are several approaches to extend the Drude-Model [2] for optical properties of metal to temperature dependence [3, 4, 5]. However, a verification of these models is difficult due to the lack of sufficient experimental data. Even though measuring optical properties with ellipsometry is well established, such measurements on metals and alloys at elevated temperatures up to the liquid state are very challenging. To collect the optical properties of different metals and alloys like Al, Ti, Ag, Cu and steel in the solid and liquid state a custom-made high-temperature ellipsometer was used. The instrument is also used to investigate the influence of curved and rough surfaces which may occur due to the heating of the samples during the ellipsometric measurements.

Introduction

There are several publications reporting on measurements of optical properties of metals from the visible spectrum up to the infrared and far infrared region at room temperature [6, 7]. The comparison of the experimental data with the Drude-Model for the optical properties of metals has revealed that the Drude model can predict the qualitative behavior of the optical properties in metal but fails to deliver the exact quantitative values. Therefore several attempts have been made to extend the Drude-model in order to predict the right values [3, 4, 5, 6, 7]. Such models include effects like the anomalous skin effect or introduce Lorentz-oscillator, which take care of resonant frequencies where the absorption is increased.

Further, experiments as well as extended Drude-models have been reported, where the temperature dependency of the optical properties of metals have been measured or calculated, respectively [4, 5, 8]. These experiments have been conducted at the wavelength of 10.6µm. This is mainly due to the interest in metal-cutting with the CO_2-laser. The extended Drude-models taking the temperature dependency into account rely on measuring the

temperature dependence of other, hard to measure parameters like the electrical conductivity or the effective electron mass of molten metals at high temperatures [4,5]. The comparison of experimental data with the temperature dependent Drude-Model shows diverging results for different metals. For example Bruckner et al. [5] reports a good agreement of theory and experiment in the case of gold. But in the case of tin they observe a larger disagreement between experiment and theory. Further a larger disagreement is reported for optical properties of metals in the liquid state, as well.

As we are mainly interested in the optical properties of liquid metals at a wavelength of 1.06µm, we have carry out our own experiments measuring the optical properties of liquid metals. In this paper, we will mainly report on the challenges to be solved when doing experiments on metals at elevated temperatures and in the liquid state. Additionally we will compare our measured data with the values from different models using spectral and temperature depending calculations.

Experimental setup

In order to measure the optical properties of metals at room temperature up to the liquid phase a custom-made ellipsometer attached to a vacuum chamber was built, as it is shown in Figure 1. Compared to absorption and reflectometry measurements ellipsometry has the advantage to measure only intensities differences and not absolute values. In the case of hot metals the black body radiation already shows a non-negligible radiation around the wavelength of interest of 1µm and therefore would distort the signal. Additionally with ellipsometry the dielectric function can be calculated. Therefore not only the total absorption and the reflection are known but the refractive index, the absorption coefficient and the angle dependence of the absorption can be calculated, as well. The ellipsometer was set up as Polarizer-Sample-Compensator-Analyzer (PSCA). For measuring the ellipsometric angles Ψ and Δ the method of Rotating Compensator Ellipsometry (RCE) was applied [7, 9, 10]. From the ellipsometric angle Ψ and Δ the dielectric function ε was calculated using the standard bulk model [7, 11].

As a light source a fiber coupled super luminescence emitting diode (SLED) was used with a center wavelength at 1070nm and a bandwidth of 100nm. The intensity of the reflected light was measured with a linearized spectrometer with a spectral range from 500nm to 1160nm.
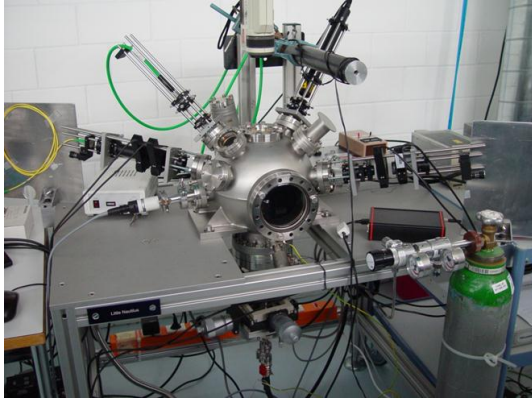

Figure 1: Vacuum chamber with the ellipsometer attached to it; the yellow fiber is the light source of the ellipsometer, the red fiber is the heating laser.

The source and the detection part of the ellipsometer were attached to two viewports of the vacuum chamber. The vacuum chamber was operated at $2 \cdot 10^{-5}$mbar. Several viewport pairs could be used for the ellipsometer resulting in different angle of incidence for the ellipsometer. For the reported data's an angle of incidence of 80°degree has been chosen. The additional viewports were mainly used for diagnostic tools. The metal samples could be heated with two different heating sources: the first heating source consisted of an electrically powered heating stage, which could heat the sample up to 1'000°C. This heating stage could be moved along the x-, y- and z-axes and be rotated along x- and z-axes. Therefore it was possible to realign the ellipsometer set-up while the metal sample was heated inside the vacuum chamber. As a second heating source a fiber coupled laser diode (LD) was use emitting at 800nm with a maximum optical output power of 350W. The two heating sources were used individually as well as in combination with each other. In combination metals and metal alloys up to melting temperatures of about 1700°C (e.g. materials like Ti and steel) could be melted.

Further the crucible materials have to be chosen carefully as liquid metal is very aggressive. Graphite crucibles were used in the case of aluminum, copper, gold and silver. Additionally molybdenum crucibles have been used in the case of silver and titanium, as well. As stainless steel reacts with graphite as well as with molybdenum the molybdenum crucible was coated with a 200µm thick ceramic layer (Al_2O_3) for steel samples.

Samples for the heating experiments were polished, pure metals square plates of 10mm length and 2mm thickness. Additionally metal coatings on polymer substrates (PET) have been used for studying the influence of rough surfaces on the ellipsometry.

Experimental issues

Curved surface

When heating the metal sample, the shape of the sample changed. Once the sample has melted, for most of the investigated materials it took a convex shape of a hemisphere with a radius of roughly 5mm. Figure 2 shows a molten aluminum sample. In order to investigate the influence of a curved surface on the ellipsometry, the refractive index and the absorption coefficient of a steel foil has been measured. Firstly the measurements have been done on the flat steel foil. Then the steel foil was bent to a cylindrical shape and the refractive index and absorption coefficient on the curved surface has been measured with the plane of incidence parallel and perpendicular to the cylindrical axes, respectively. As table 1a shows, there is no difference in the refractive index and absorption coefficient between the flat and the curved steel foil, respectively.

Steel foil	n	k
flat	3.49	5.07
bend, 10mm diameter	3.42	5.09

Table 1a: refractive index *n* and absorption coefficient *k* for a flat and a bend steel foil, respectively.

Further, ellipsometric measurements on steel ball bearing with different diameter have been conducted, using ball diameters of 7.5mm, 10mm and 12.5mm. As it is shown in table 1b, no significant difference between the different diameters can be detected. Therefore it can be assumed that curved surface have no influence on the ellipsometric measurements. Note that the differences between the values for the steel foil and the ball bearing are due to a different composition of the two steel samples.

Steel ball bearing	n	k
7.5mm diameter	3.29	4.67
10mm diameter	3.24	4.62
12.5mm diameter	3.25	4.60

Table 1b: refractive index *n* and absorption coefficient *k* for a steel ball bearing with different ball diameter, respectively.

Additionally the experiments on curved surfaces have shown that it is very important to realign the curved samples correctly. Aligning the ellipsometer with flat sample surfaces is mainly done by finding the maximum signal for a neutral polarizer position. This procedure is not accurate in the case of curved sample surfaces. Relative maxima of the signal can be detected even though the light beam of the

ellipsometer is not reflected at the top of the hemisphere but on the side of it. Therefore a HeNe-laser as a guide laser was used to accurately realign the curved sample surface once the metal was melted.
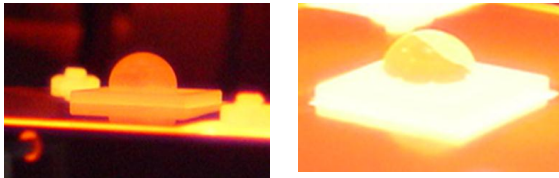
Debris

Figure 2: The left picture show a liquid aluminum sample just above the melting point with a homogenous looking surface; the right picture shows the same sample well above the melting point with two distinguishable surface areas.

When heating the metal samples just above the melting point the surface of the metal hemisphere appeared smooth, as it is shown in the left picture of Figure 2. Nevertheless repeated measurements of the refractive index and the absorption coefficient at the same spot revealed a large scattering of the values. When the samples were heated well above the melting points, the liquid metal surface cracked showing a brighter and a darker area on the surface, as it is shown on the right picture in Figure 2. Measurements on both areas revealed that the brighter areas still show the same large scattering in the values of the refractive index and absorption coefficient whereas the darker areas showing a similar scattering compared to the measurement on the solid metal sample. The dark areas were identified as the pure liquid metal whereas the bright areas contain some sort of debris. For the measurement it is important that there is no debris on the top of the hemisphere of the liquid metal sample. By pointing the heating laser at the right spot (i. e. pointing somewhat to the side of the hemisphere) it is possible to "push" the debris to the side.

Roughness

It is well known in ellipsometry and surface science that the surface topography has a strong influence on the reflectivity [12, 13 14, 15, 16]. There exist different approaches to describe the influence of a rough surface on the ellipsometric measurement. Unfortunately they are inaccurate in the case of metal surfaces. In order to estimate the influence of rough surfaces on our measurements metal surface samples with different roughness have been prepared and measured. The samples have been prepared by plasma treating polymer substrates for different time periods resulting in different roughness [17]. Then the substrates were coated with silver or gold metal layers of about 200µm thickness, respectively. The R_a roughness values have been measured by atomic force microscopy.
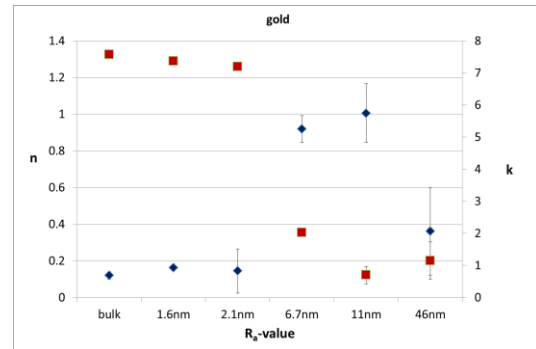

Figure 3a: refractive index n and absorption coefficient k of gold as a function of surface roughness R_a;
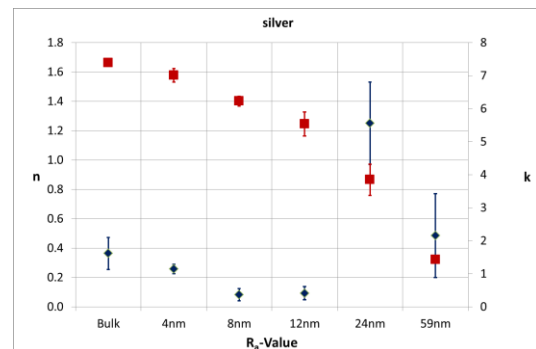

Figure 3b: refractive index n and absorption coefficient k of silver as function of surface roughness R_a.

In this way rough sample surfaces have been prepared with R_a-values from approx. 1nm to 60nm. In the case of gold as well as silver for small R_a-values up to 4nm n and k correspond to the value of the polished bulk measurement. Above $R_a=4nm$ for both metals n and k are different from the values of the well-polished bulk sample. Additionally the error bar is increasing as well. It has to be pointed out that the values shown in the figure 3a and 3b for roughness above $R_a=4nm$ are not the real values for n and k that a light beam "sees" at that surface. The values are calculated from the ellipsometric angles Ψ and Δ still assuming well-polished bulk material with a perfectly smooth surface. The change in n and k indicates that the ellipsometric angles Ψ and Δ have changed, meaning the surface condition for reflecting polarized light does not correspond to that of a polished bulk surface. For calculating the appropriate values for n and k the bulk model has to be adapted. Unfortunately, as mentioned above, there exists no such adaption of the ellipsometric theory for rough metal surfaces. Nevertheless from the experimental point of view this experiment clearly shows that surface roughness has a great influence on the ellipsometric measurement and it is crucial that the measurement are conducted on smooth sample surfaces. In the case of solid samples the surface is well polished. Unfortunately, due to heating the surface structure of the samples changes. For example in the case of steel when the sample is heated up from room temperature to above 1'000°C, its surface changes from smooth to

a satin like surface, showing all tempering color, back to a smooth, mirror like surface.

Theoretical calculations

Temperature depending Drude-Model

The general theory of optical constants of metals assumes a free electron gas in metals, as it was first introduced by Paul Drude [2]. For the temperature dependency of the Drude-model we mainly follow the paper of Bruckner et al [4, 5]. In these references the anomalous skin effect [18] is included into the Drude-model and the model is tested with experimental results from ellipsometry with a CO_2 Laser at $10.6\mu m$ as a light source. According to Bruckner et al. the dielectric function of the Drude-model is given by:

$$\varepsilon_D(\omega) = \varepsilon_1(\omega) - i\varepsilon_2(\omega), \text{ where} \tag{1}$$

$$\varepsilon_1(\omega) = 1 - \frac{\sigma_0\tau}{\varepsilon_0} \frac{1}{\left[1 + (\omega\tau)^2\right]}, \text{ and} \tag{2}$$

$$\varepsilon_2(\omega) = \frac{\sigma_0}{\varepsilon_0\omega\left[1 + (\omega\tau)^2\right]} \tag{3}$$

The σ_0 is the dc conductivity and the ω is the frequency of light. Further τ is the collision time for electrons having nearly Fermi's energy related to σ_0:

$$\tau = \frac{\sigma_0 m_e^*}{n_e e^2} \tag{4}$$

where n_e is the electron density. The m_e^* is the so-called effective electron mass, which takes the deformation of the Fermi sphere in real solid bodies due to the ionic potential trunks into account. The electron density is given by:

$$n_e = N_{val} \frac{\rho}{u} \tag{5}$$

where N_{val} is the number of electrons in the valence-band, ρ is the mass density of the metal and u is the molecular weight of the metal.

From the dielectric function the refractive index n and the absorption coefficient k can be calculated:

$$n = \text{Re}\left(\sqrt{\varepsilon}\right), \text{ and} \tag{6}$$

$$k = \text{Im}\left(\sqrt{\varepsilon}\right) \tag{7}$$

Taking account of the anomalous skin effect a small term can be added to n and k, respectively:

$$\Delta n = \frac{3v_F}{16c_0} \frac{k^2 - \frac{2nk}{\omega\tau} - n^2}{1 + \left(\frac{1}{\omega\tau}\right)^2} \tag{8}$$

$$\Delta k = \frac{3v_F}{16c_0} \frac{\frac{n^2 - k^2}{\omega\tau} - 2nk}{1 + \left(\frac{1}{\omega\tau}\right)^2} \tag{9}$$

where v_F is the so called Fermi's velocity and c_0 is the speed of light in vacuum.

The material parameters σ_0 and ρ (therefore τ and n_e as well) depend on the temperature and m* on the phase of the metal. Therefore n and k can be calculated as a function of the temperature.

Drude-Model with Lorentz-oscillator

The Drude-model can qualitatively explain some optical properties of metals and by taking the anomalous skin effect into account, it is possible to calculate the optical parameters for some metals and wavelengths, especially for longer wavelengths in the IR. Nevertheless the Drude-model does not take into account any resonant frequencies where the absorption significantly increases. Therefore it fails to correctly predict the optical properties of metals at shorter wavelengths in the Near-IR and the visible range. By extending the Drude-model with a Lorentz-oscillator the resonant frequency absorption can be included. According to Rakic et al [6] the general dielectric function can be written as:

$$\varepsilon_L(\omega) = \varepsilon_{free}(\omega) + \varepsilon_{band}(\omega) \tag{10}$$

where $\varepsilon_{free}(\omega)$ is the intra-band term based on the free electron approach of the Drude-model given by:

$$\varepsilon_{free}(\omega) = 1 - \frac{\Omega_p^2}{\omega(\omega - i\Gamma_0)}, \text{ where} \tag{11}$$

$$\Omega_p = \sqrt{f_0}\,\omega_p \tag{12}$$

is the plasma frequency associated with the intra-band transition with the oscillator strength f_0 and the damping constant Γ_0. It can easily be shown that dielectric function $\varepsilon_{free}(\omega)$ of the equation (9) and (10) is related to the $\varepsilon_D(\omega)$ defined by the equations (1)-(3). The $\varepsilon_{band}(\omega)$ is the inter-band term based on Lorentz-oscillator for insulators given by:

$$\varepsilon_{band}(\omega) = \sum_{j=1}^{n_{oc}} \frac{f_j \omega_p^2}{\omega_j^2 - \omega^2 + i\omega\Gamma_j} \qquad (13)$$

where n_{oc} is the number of oscillators with the resonant frequency ω_j, the oscillator strength f_i and the lifetime $1/\Gamma_j$. Further ω_p is the plasma frequency given by:

$$\omega_p^2 = \frac{4\pi n_e e^2}{m_e}, \qquad (14)$$

where m_e is the electron mass and e is the electron charge. Here as well, the electron density n_e is a function of the temperature. Additionally the resonant frequency ω_j, the oscillator strength f_i and the lifetime $1/\Gamma_j$ are temperature depending as well. Unfortunately we do not have any knowledge in what way they vary with temperature change. Therefore, for a first approach the only temperature depending parameter is the electron density n_e for calculating $\varepsilon_L(\omega)$.

Combined calculations

Both models have been combined by replacing the intra-band term $\varepsilon_{free}(\omega)$ in equation (10) with the temperature depending dielectric function $\varepsilon_D(\omega)$ of the equations (1)-(3). Additionally corrections for n and k due the anomalous skin effects according the equations (8) and (9) are included, as well.

Results and discussion

The following section compares the refractive index n and the absorption coefficient k of our own measurement with the calculated values for gold and silver, respectively. The theoretical values were calculated using the temperature depending Drude-Model as described by Bruckner et al [4, 5], the Lorentz-model explained by Rakic et al [6, 7] and the combined calculation as described in the previous section. In the appendix the material parameters used in the calculations are listed.

Gold

Figure 4a and 4b show the refractive index n and the absorption coefficient k of gold as a function of the temperature, respectively.

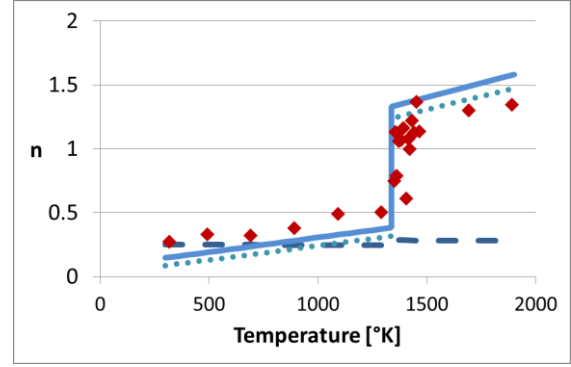Fig. 4a: refractive index n of gold as a function of the temperature; comparing measurement (red diamonds) with calculated values Drude (blue dotted line), Lorentz (blue dashed line) and combined model (red straight line)
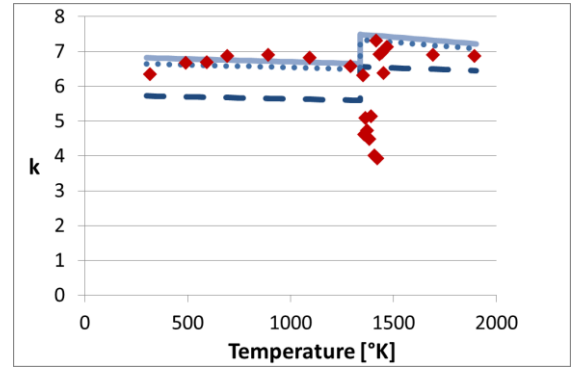

Fig. 4b: absorption coefficient k of gold as a function of the temperature; comparing measurement (red diamonds) with calculated values Drude (blue dotted line), Lorentz (blue dashed line) and combined model (blue straight line)

The Drude-model and therefore the combined model predict a discrete step of the refractive index n and the absorption coefficient k at the phase transition. Additionally the refractive index n increases with increasing temperature in the solid as well in the liquid phase. The experimental results confirm this temperature behavior of n and k for gold. In opposite to that the Lorentz-model according to Rakic et al [6] where the change of n and k at the phase transition is less pronounced. This is mainly due to the missing knowledge of the temperature dependencies of the oscillator strength f_i and damping constants Γ_i.

Further the experimental results of the k clearly show the influence of the debris on the surface of the liquid metal sample. The cracking up of this debris layer only starts at higher temperatures well above the melting point. Additionally during the heating of the gold sample below the melting point the surface of the sample changed from a smooth surface to a satin like surface and back to smooth again. This change in surface structure is reflected by the k-value. The models show a linear behavior between the k-value and the temperature whereas the experimental results show a hump.

Silver

Figure 5a and 5b show the refractive index *n* and the absorption coefficient *k* of silver as a function of the temperature, respectively.
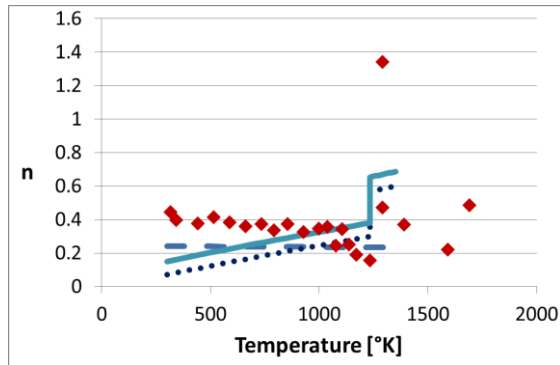

Fig. 5a: refractive index *n* of silver as a function of the temperature; comparing measurement (red diamonds) with calculated values Drude (blue dotted line), Lorentz (blue dashed line) and combined model (blue straight line)

Fig. 5b: absorption coefficient *k* of silver as a function of the temperature; comparing measurement (red diamonds) with calculated values Drude (blue dotted line), Lorentz (blue dashed line) and combined model (blue straight line)
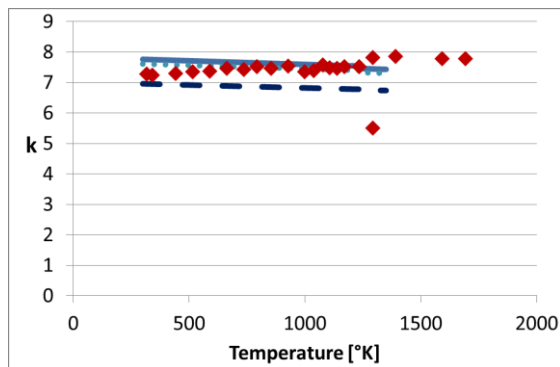
In the same way as with gold the Drude-model predicts a discrete jump of the refractive index *n* for the phase transition of silver. But in opposite to gold this behavior is not confirmed by our experimental data. The Lorentz-model seems to be more accurate in this case. Moreover the experimental value of the refractive index *n* decreases with increasing temperature below the melting point as it is predicted by the Lorentz-model, but not by the Drude-model.

Summary

We have reported on measuring the optical properties of metal from room temperature up to above the melting point of different metals. Due the heating of the sample the sample surface is changing constantly. It has been shown that the change in surface curvature does not have a measurable influence on the optical properties. Nevertheless it is very important to realign the ellipsometer on the right spot of a curved surface sample. On the other hand a strong influence can be detected for the change of surface roughness and for the accumulation of debris on the liquid metal surface. In the case of the debris accumulation it is important to conduct the experiment inside a vacuum chamber and therefore minimize the debris. Furthermore it is important to heat the sample well above the melting point. This will cause the debris layer to crack up. With a clever heating strategy the debris could be "pushed" to the side. Concerning surface roughness it is important that well-polished, always in the same way prepared samples are used. Nevertheless once the surface of the sample changes during the heating of the sample, there is not much which can be done against it. Therefore results on such surfaces have to be treaded cautiously.

Comparing the experimental results with different theoretical models has revealed that currently there is no general approach which describes the temperature behavior of the optical properties correctly for all metals. For example in the case of gold the approach of relating temperature dependency of the dielectric function to the temperature dependency of the electrical conductivity predicts the experimental data correctly. Especially the discrete change of the refractive index *n* and absorption coefficient *k* at the phase transition is reflected correctly. However in the case of silver the Drude-model shows an increasing of the refractive index *n* and absorption coefficient *k* with increasing temperature with a discrete change at the transition of phase as well. But in opposite to gold this behavior cannot be seen in the experimental results of silver. According to our own findings silver shows a small or no temperature dependency of the optical properties *n* and *k*. In general for all the measured metals a weaker temperature dependency has been measured than the temperature depending Drude-model predicts.

In summary due to the lack of a general model one is urged to measure the temperature depending optical properties of each metal and metal alloy separately. Further the different models make use of other material properties like electrical conductivity, resonant frequency or oscillator strength. To measure these parameters as a function of temperature well above the melting point is sometimes even more challenging than to measure the optical properties directly.

Appendix: material parameters

The volume expansion and the electrical resistivity as a function of the temperature are given as a polynomial [19, 20, 21]:

$$f(T) = a_0 + a_1 \cdot T + a_2 \cdot T^2$$

A comprehensive summery of the presented material parameters and additional metals can be found in Pottlacher [22]. The additional material parameters are taken from the CRC Handbook of Chemistry and Physics [23]

Gold

Volume expansion V/V_0 [19]:

Temperature range: 1337 K < T < 4300 K
a_0: 1.0265
a_1: 6.1608 x 10^{-5}
a_2: 1.1306 x 10^{-8}

Density at 20 °C [23]:

ρ=19300 kg·m^{-3}

Electrical resistivity in $\mu\Omega \cdot m$ [19]:

Temperature range: 1337 K < T < 4300 K
a_0: 0.1473
a_1: 1.1270 x 10^{-4}
a_2: 2.09539 x 10^{-8}

Fermi Deformation m^*/m_e [5]:

solid: $\dfrac{m^*}{m_e} = 1.3$

liquid: $\dfrac{m^*}{m_e} = 0.99$

Lorentz oscillator [6, 7]:

	i=0	i=1	i=2	i=3	i=4	i=5
f_i	0.760	0.024	0.010	0.071	0.601	4.384
Γ_i	0.053	0.241	0.345	0.870	2.494	2.214
ω_i	---	0.415	0.830	2.969	4.304	13.32

where Γ_i and ω_i are in Electronvolt.

Silver

Volume expansion V/V_0 [20]:

Temperature range: 1234 K < T < 2000 K
a_0: 1.002
a_1: 4.736 x 10^{-4}
a_2: 0

Density at 20 °C [23]:

ρ=10500 kg·m^{-3}

Electrical resistivity in $\mu\Omega \cdot m$ [21]:

Temperature range: 1234 K < T < 2000 K
a_0: 0.0554
a_1: 8.3336 x 10^{-5}
a_2: 0

Fermi Deformation m^*/m_e

No values could be found for silver.

Lorentz oscillator [6, 7]:

	i=0	i=1	i=2	i=3	i=4	i=5
f_i	0.845	0.065	0.124	0.011	0.840	5.646
Γ_i	0.048	3.886	0.452	0.065	0.916	2.419
$\omega_{i\,i}$	---	0.816	4.481	8.185	9.083	20.29

where Γ_i and ω_i are in Electronvolt.

References

1 H. Hügel, T. Graf (2009), Laser in der Fertigung, Viewweg+Teubner, ISBN 978-8351-0005-3

2 P. Drude (1900), Zur Elektronentheorie der Metalle, Annalen der Physik 306 (3), 566–613.

3 V. I. Konov, V. N. Tokarev (1983), Temperature dependence of the absorptivity of aluminum targets at the 10.6μm wavelength, Sov. J. Quantum Electron., 13(2) Feb., 177-180.

4 M. Brückner, J. H. Schäfer, J. Uhlenbusch (1989), Ellipsometric Measurement of the Optical Constants of Solid and Molten Aluminum and Copper at λ=10.6μm, J. Appl. Phys. 66(3) Aug., 1326-1332.

5 M. Brückner, J. H. Schäfer, C. Schiffer, J. Uhlenbusch (1991), Measurement of the optical constants of solid and molten gold and tin at λ=10.6μm, J. Appl. Phys. 70(3) Aug., 1642-1647.

6 A. D. Rakic, A. B. Djurisic, J. M. Elazar, M. L. Majewski (1998), Optical properties of metallic films for vertical-cavity optoelectronic devices, Appl. Opt. 37(22) August, 5271-5283.

7 H. Fujiwara (2009), Spectroscopic Ellipsometry, John Wiley & Sons Ltd., ISBN 978-0-470-01608-4,

8 F. Dausinger (2005), Strahlwerkzeug Laser: Energiekopplung und Prozesseffektivität, in series Laser in der Materialbearbeitung

Forschungsberichte des IFSW, Institut für Strahlwerkzeug, Stuttgart.

9 R. Kleim, L. Kuntzler, A. El Ghemmaz, Systematic errors in rotating-compensator ellipsometry (1994), J. Opt. Soc. Am. A 11(9) September, 2550-2559.

10 I. An, J. A. Zapien, C. Chen, A. S. Ferlauto, A. S. Lawrence, R. W. Collins (2004) Thin Solid Films 455-456, 132-137.

11 H. G. Tompkins, E. A. Irene(2005), Handbook of Ellipsometry, William Andrew publishing, Springer, ISBN 3-540-22293-6 or 0-8155-1499-9.

12 B. Lehner, K. Hingerl (2004), The finite difference time domain method as a numerical tool for studying the polarization optical response of rough surfaces, Thin Solid Films 455-456, 462-467.

13 V. Sirtori, L. Magagnin, E. Saglia, P. L. Cavalloti (2004), Calculation model of rough gold optical constant, Surface Science 554, 119-124.

14 S. N. Svitasheva (2011), Random phase mask as a model of rough surface. Part I Theory, Thin Solid Films 519, 2718-2721.

15 S. N. Svitasheva (2011), Random phase mask as a model of rough surface. Part II Experiment, Thin Solid Films 519, 2722-2724.

16 L. V. Poperenko, V. S. Voitsenya, M. V. Vinnichenko, V. G. Konovalov, O Motojima, K. Sato, A. Sagara, K. Tsuzuki (1999), Optical effects of metallic mirror surface modification, Surface and Coatings technology 114, 200-205.

17 T. Smith (1976), Effect of Surface Roughness on Ellipsometry of Aluminum, Surface Science 56, 252-271

18 P. W. Gilbert (1982), The anomalous skin effect and the optical properties of metals, J. Phys. F: Met. Phys. 12, 1845-1860.

19 E. Kaschnitz, G. Nussbaumer, G. Pottlacher, H. Jäger (1993), Microsecond-resolution measurements for the investigation of liquid gold, Int. J. of Thermophysics 14(2), 251-257.

20 T. Hüpf, C. Cagran, G. Pottlacher (2010), Thermophysical properties of 22 pure metals in the solid and liquid state – the pulse-heating data collection, Lam14 Conference Proceedings.

21 C. Cargan, B. Wilthan, G. Pottlacher (2006), Enthalpy, heat of fusion and specific electrical resistivity of pure silver, pure copper and the binary ag-28cu alloy, Thermochimica Acta 445, 104-110.

22 G. Pottlacher (2010), High Temperature Thermophyscal properties of 22 Pure Metals, edition keeper, ISBN 978-3-9502761-6-9.

23 D. R. Lide (editor), CRC Handbook of Chemistry and Physics. CRC Press LLC (2004)